

Self-consistent model of magnetoplasmons in quantum dots with nearly parabolic confinement potentials

Vidar Gudmundsson

Science Institute, University of Iceland, Dunhaga 3, IS-107 Reykjavik, Iceland

Rolf R. Gerhardt

*Max-Planck Institut für Festkörperforschung, Heisenbergstrasse 1,
D-7000 Stuttgart 80, Federal Republic of Germany*

(Received 14 February 1991)

We investigate the longitudinal collective oscillations of a two-dimensional interacting electron gas (2DEG) confined to a disk (quantum dot) in a perpendicular constant magnetic field. We show how the exact results known for a parabolically confined 2DEG change when the confining potential and the electron number are varied. Considering reasonable corrections to a parabolic confinement potential, we are able to explain all features of the far-infrared spectrum of quantum dots observed in recent experiments.

The dispersion of magnetoplasmons in a two-dimensional electron gas (2DEG) confined to a circular disk has been measured by several groups¹⁻³ and is well described by the simple formula

$$\omega_{\pm} = \frac{1}{2}(\tilde{\omega} \pm \omega_c), \quad \tilde{\omega} = (\omega_c^2 + 4\omega_0^2)^{1/2}, \quad (1)$$

where $\omega_c = eB/mc$ is the cyclotron frequency of an electron of effective mass m in a perpendicular homogeneous magnetic field B . For large disks, ω_0 has been interpreted as a plasmonic frequency.^{1,3-5} For small "quantum dots," ω_0 has been related to a parabolic confinement potential, $V_{\text{conf}}(\mathbf{r}) = \frac{1}{2}m\omega_0^2 r^2$, and the insensitivity of the measured dispersion to the number N of electrons in the quantum dot has been interpreted as indication for a suppression of many-body effects.² In recent high-resolution experiments on larger quantum dots in GaAs heterostructures with 25 and more electrons per dot, Demel *et al.*³ observed an additional resonance with a frequency ω'_+ above the ω_+ of Eq. (1) at high magnetic fields ($B \geq 5$ T), and an anticrossing-type splitting of the ω_+ resonance at smaller fields ($B \approx 1.2$ T). The upper mode ω'_+ could be fitted by Eq. (1) using a plasma frequency $\omega'_0 > \omega_0$, and the anticrossing was attributed to a nonlocal interaction of the corresponding ω'_- mode with the ω_+ mode.^{3,5} The physical mechanism which makes the higher mode and the anticrossing observable is, however, not yet understood.

Recently it has been realized that the dispersion relation (1) gives the exact far-infrared (FIR) resonance frequency for dots with an arbitrary number of interacting electrons, if the confinement potential is parabolic and the FIR electric field radiated into the system is homogeneous over the dot size.^{6,7} Then, the center-of-mass (CM) motion decouples from the relative motion (RM) of the electrons in the dot. The homogeneous external electric field excites only the CM motion which has precisely the

same energy eigenvalues, and thus the same dipole resonance frequencies, as a single electron. The more complicated resonance structures observed by Demel *et al.*³ on a quadratic array with many ($\sim 10^4$) dots must, therefore, be attributed to either interaction effects between different dots or to a nonparabolic confinement potential for a single dot. Both perturbative methods⁷ and exact diagonalization for few-electron systems⁸ have shown that the interaction between dots decreases rapidly with increasing dot separation and is unimportant for the experimental situation.³ Deviations from parabolic confinement change the dipole selection rules for the CM motion and, more importantly, couple the CM and the relative motion of the electrons in the dot. In this Rapid Communication we want to demonstrate that a circular symmetric correction (e.g., $\propto r^4$) to the confinement potential explains already the occurrence of a higher mode and a weak N dependence of the main resonance frequency, as observed in experiment.³ To understand the anticrossing, we have to assume that the dots are not strictly circular symmetric. A correction to the confinement potential with square symmetry [e.g., $\propto (x^4 + y^4)$], which in view of the preparation procedure is likely to exist in the investigated dot systems,³ leads to the observed anticrossing behavior.

Our arguments are based on numerical calculations for circular symmetric dots and on an analytic, perturbative treatment of deviations from the parabolic confinement. Here we can present only the basic ideas and main results, details are left for a future publication. The numerical calculations treat the ground state of the interacting electrons ($10 \leq N \leq 30$) in a dot in the Hartree approximation⁹ and the FIR response in the random-phase approximation (RPA). In the following we assume a strong quantum confinement in the z direction parallel to the magnetic field and perpendicular to the

plane of the dots, and we neglect the extent of the electronic wave functions in the z direction. For an electron confined in a circular symmetric potential $V_{\text{conf}}(r)$ and with gauge $\mathbf{A} = \frac{1}{2}B(-y, x, 0)$, the angular momentum $L_z = xp_y - yp_x = -i\hbar\partial/\partial\varphi$ is conserved with eigenvalues $-\hbar M$ and the energy eigenfunctions are, in polar coordinates, of the form $\psi(r, \varphi) = \exp(-iM\varphi)\Phi_{Mn}(r)$ ($M = 0, \pm 1, \dots$). For $V_{\text{conf}}(r) = \frac{1}{2}m\omega_0^2 r^2$, the eigenfunctions and energies E_{Mn} are well known,^{6,10}

$$\Phi_{Mn}(r) \propto \lambda^{-1} u^{|M|/2} e^{-u/2} L_n^{|M|}(u), \quad u = \frac{r^2}{2\lambda^2}, \quad (2)$$

with $L_n^{|M|}$ a Laguerre polynomial, $\lambda^2 = \hbar/m\tilde{\omega}$, and $2E_{Mn}/\hbar = (2n+|M|+1)\tilde{\omega} - M\omega_c$ ($n = 0, 1, \dots$). States

$$\chi^{2D}(\mathbf{r}, \mathbf{r}') = \sum_{M, n, M', n'} \Phi_{Mn}(r) \Phi_{M'n'}(r) \Phi_{Mn}(r') \Phi_{M'n'}(r') e^{-i(M-M')(\varphi-\varphi')} \frac{f_{Mn} - f_{M'n'}}{\hbar\omega + E_{Mn} - E_{M'n'} + i\eta}, \quad (3)$$

where f_{Mn} is the Fermi occupation number of the single-particle state with energy E_{Mn} , and $\eta \rightarrow 0^+$. To simulate the FIR response of the dot, we calculate the linear response to an external *longitudinal* (nonpropagating) time dependent electric field $\mathbf{E}^{\text{ext}} = -\nabla\phi^{\text{ext}}$. Within the RPA, this leads to a self-consistent potential $\phi^{\text{sc}} = \phi^{\text{ext}} + \phi^{\text{ind}}$ which, in the plane $z = 0$ of the dot, satisfies the integral equation

$$\phi^{\text{sc}}(\mathbf{k}) = \phi^{\text{ext}}(\mathbf{k}) + \frac{2\pi e^2}{\kappa} \int d^2q \chi^{2D}(\mathbf{k}, \mathbf{q}) \phi^{\text{sc}}(\mathbf{q}), \quad (4)$$

where planar Fourier transforms are taken. Knowing the solution, we can calculate the power absorption from the Joule heating,

$$P(\omega) = -\frac{\omega}{8\pi} \int \frac{d^2k}{(2\pi)^2} |\phi^{\text{ext}}(\mathbf{k})|^2 \text{Im} \left(\frac{\phi^{\text{sc}}(\mathbf{k})}{\phi^{\text{ext}}(\mathbf{k})} \right), \quad (5)$$

with a small finite value of η ($=0.03\hbar\tilde{\omega}$) in Eq. (3) to get resonance lines of finite width. Collective modes (magnetoplasmons), defined as nontrivial solutions of Eq. (4) for $\phi^{\text{ext}} = 0$, show up as resonance peaks in $P(\omega)$.

Due to the circular symmetry of the system the eigenmodes have a well defined angular momentum, $\phi^{\text{sc}}(\mathbf{r}, z = 0) = \phi^{\text{sc}}(r) \exp(-iN_p\varphi)$ as is seen from Eq. (3). Thus, in the Fourier transforms, $\phi^{\text{ext}}(\mathbf{q}, 0) = \phi^{\text{ext}}(q) \exp(-iN_p\varphi_q)$, we choose $\phi^{\text{ext}}(q) = Q^{N_p} \exp(-\beta Q^2)$ with $Q = \sqrt{2}\lambda q$, so that for $N_p = \pm 1$ the external field has circular polarization and, in the limit $\beta \rightarrow \infty$, induces dipole transitions in the dot. For the numerical calculations we take $\beta = 60$, choose GaAs parameters, $m = 0.067m_0$, $\kappa = 12.4$, and calculate $P(\omega)$ for three different confining potentials of the form

$$V_{\text{conf}}(r) = ar^2 + br^4 + cr^6, \quad (6)$$

with $a = 50 \times 10^{-6} \text{ meV}/\text{\AA}^2$. For $b = c = 0$, this is a parabolic confinement with $\hbar\omega_0 = 3.37 \text{ meV}$ and, for $N=30$, the electron density profile we calculated has a radius of approximately 10^3 \AA . For both $N_p=1$ and $N_p = -1$ we find in this case a single peak of $P(\omega)$

with $M(> 0)$ and $-M$ have the same radial wave function with mean square radius $r_{Mn}^2 = 2\lambda^2(2n+|M|+1)$, but the energy of the $-M$ state is by $M\hbar\omega_c$ higher. For N interacting electrons in this parabolic confinement potential, the CM moves just as an electron with N -fold mass and N -fold charge,^{6,7} i.e., with the same energy eigenvalues and eigenfunctions, but with a smaller amplitude, $\lambda^2 \rightarrow \lambda_{\text{CM}}^2 = \lambda^2/N$. In the Hartree approximation, we do not exploit this knowledge and calculate the Φ_{Mn} and E_{Mn} self-consistently, together with the electron density $n_e(r)$ and the resulting Hartree potential $V_H(r)$, which adds to $V_{\text{conf}}(r)$ in Schrödinger's equation.⁹ Using the self-consistent potential, we calculate the density-density response function

from which the dispersion relations of Fig. 1 are obtained. Thus, our consistent Hartree-RPA approach reproduces the exact results for parabolic confinement very well. We also find that the resonance spectrum is independent of the electron number N , as it should. This is demonstrated in Fig. 2 for $B=0$. Similar results were recently obtained by Broido and co-workers,^{11,7} whereas a RPA calculation which neglects the Coulomb interaction in the ground state predicts strong N -dependent frequency shifts.¹²

We also investigated corrections to the parabolic confinement by putting in Eq. (6) (a) $b = 10^{-11} \text{ meV}/\text{\AA}^4$ and $c = 0$, and (b) $b = 0$ and $c = 10^{-17} \text{ meV}/\text{\AA}^6$. In both cases the resonance spectrum becomes weakly N -dependent, as is demonstrated for the $N_p = 1$ mode and $B = 0$ in Fig. 2. Moreover, for $B \geq 1.5 \text{ T}$ the $N_p = -1$ mode shows a splitting. The dispersion of the main peak is indicated in Fig. 3 by the full circles, that of the additional low-intensity side peak by open circles.

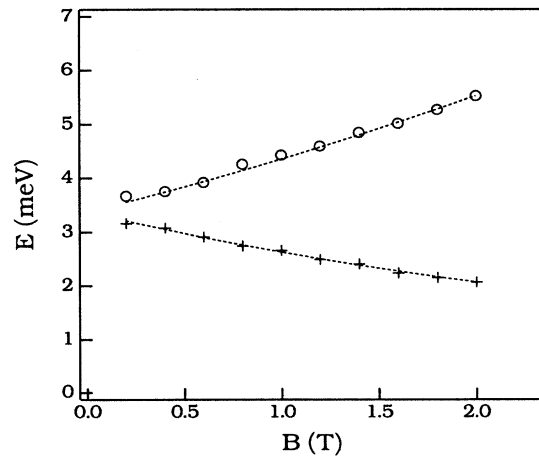


FIG. 1. The excitation spectrum in the case of parabolic confinement and an external dipole field. \circ : the $N_p = -1$ and $+$: the $N_p = +1$ mode from the calculation. The dashed lines are the exact results $\Delta E_{\pm} = \hbar\omega_{\pm}$.

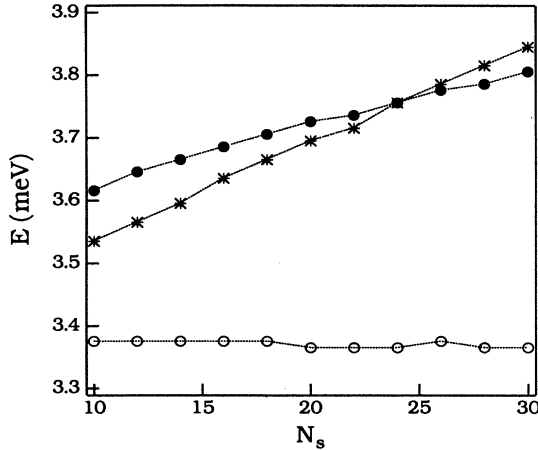


FIG. 2. The excitation spectra for $B = 0.0$ T and $N_p = +1$ as a function of the electron number N in the case of the following: \circ , parabolic confinement; \bullet , $ar^2 + br^4$; and $*$, $ar^2 + cr^6$ confinement. Values for a , b , and c are in text.

This structure continues to higher B values than shown in Fig. 3. A slight increase of the $B = 0$ resonance frequency with increasing N was also obtained by Broido, Kempa, and Bakshi.¹¹ An additional resonance was, however, not found, probably because the corresponding calculation was done for too few electrons ($N = 6$), so that the deviation from the parabolic confinement potential did not become effective.

For a deeper understanding of the RPA results, we consider the symmetry of the system. For N electrons in a circular symmetric parabolic confinement potential, the energy eigenstates can be taken as products $|M, n; l, \alpha\rangle = |M, n\rangle|l, \alpha\rangle$ of eigenstates $|M, n\rangle$ and $|l, \alpha\rangle$ of energy and angular momentum of the CM and the RM, respectively, and they are eigenstates of the total angular momentum

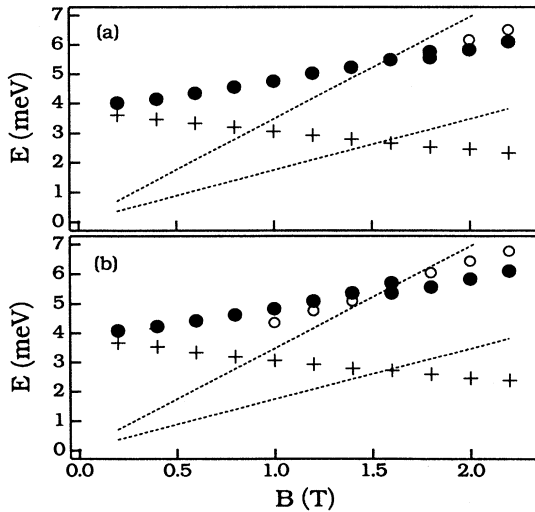


FIG. 3. The dipole excitation spectrum in the case of (a) $ar^2 + br^4$ and (b) $ar^2 + cr^6$ confinement. Position of strong (\bullet) and weak (\circ) absorption peaks for the $N_p = -1$ mode and of the peaks for the $N_p = +1$ mode ($+$) from the calculation. The dashed lines are $\omega = 2\omega_c$.

with eigenvalue $-\hbar(M+l)$. This holds with and without the Coulomb interaction, $v(\mathbf{r}_i - \mathbf{r}_j) = e^2/\kappa|\mathbf{r}_i - \mathbf{r}_j|$, which acts only on the RM. In general, the Coulomb repulsion is less effective in more extended states, and, e.g., the ground state $|l_0, \alpha_0\rangle$ of the RM occurs with increasing B at increasingly positive l_0 values.⁸ A correction br^4 to the confinement potential adds a perturbation

$$\Delta H = b \sum_{j=1}^N r_j^4 = bNR^4 + H_{22} + H_{13} + H_{04} \quad (7)$$

to the Hamiltonian H , which has nonzero matrix elements only between states with the same total angular momentum. The terms $H_{\mu,\nu}$ are of order μ in CM coordinate $\mathbf{R} = \sum_{j=1}^N \mathbf{r}_j/N$ and of order ν in the relative coordinates $\mathbf{r}'_j = \mathbf{r}_j - \mathbf{r}_1$ ($j = 2, 3, \dots, N$). In principle, the first term, bNR^4 , which affects only the CM motion, yields already a blue shift of the fundamental dipole transitions and a coupling of the dipole active state $|1, 0\rangle$ to the inactive higher state $|1, 1\rangle$. However, for reasonable values of the blue shift, the oscillator strength of the additional higher mode comes out much too small. Moreover, the matrix elements $\langle M', n'|bNR^4|M, n\rangle$ scale with increasing electron number N as $N\lambda_{\text{CM}}^4 \propto N^{-1}$ and become small, whereas the eigenvalues of the unperturbed CM Hamiltonian are independent of N .

The next term of Eq. (7), H_{22} , is the sum of two contributions. One couples states $|M, n; l, \alpha\rangle$ differing in both angular momentum quantum numbers M and l by two units, $\Delta M = -\Delta l = \pm 2$. The other,

$$H_{22}^0 = 2bNR^2 \left[\frac{1}{N} \sum_{j=2}^N r_j'^2 - \left(\frac{1}{N} \sum_{j=2}^N r_j' \right)^2 \right], \quad (8)$$

couples only states with the same M and the same l . The CM parts of its matrix elements, $\langle M', n'|2bNR^2|M, n\rangle$, are independent of N . The matrix elements of the term in square brackets in Eq. (8) with the RM states $|l, \alpha\rangle$ can be estimated to be of the order r_F^2 , the mean square radius at the Fermi energy. We estimate this for noninteracting electrons at $B = 0$, and obtain $r_F^2 = E_F/m\omega_0^2 \propto N^{1/2}$. In the subspace of states $|M, n; l_0, \alpha_0\rangle$ with $|l_0, \alpha_0\rangle$ the ground state of the RM, which is sufficient to calculate the corrections to the dipole transitions from the ground state to first order, H_{22} acts on the CM motion just as an additional parabolic confinement potential. As a consequence, we get a blue shift ($\propto N^{1/2}$) of the resonance frequencies, but no additional mode. If we consider a correction $\propto r^6$ to the parabolic confinement potential and use the same type of arguments, we obtain a blue shift proportional to N . This qualitatively explains the RPA results shown in Fig. 2. In second-order perturbation theory, H_{22}^0 leads to a higher mode, but also $H_{22} - H_{22}^0$ and H_{13} come into play, and the calculations become rather cumbersome. There is, however, no doubt that circular symmetric deviations from the parabolic confinement lead to additional dipole transitions.

To understand the anticrossing,³ we need a state with

an energy dispersion which crosses that of the dipole active state $|-1, 0; l_0, \alpha_0\rangle$ near $B = 1.2$ T. Obvious candidates are those with a CM part $|M, 0\rangle$ where $M \geq 2$. For $M=2$, the energy crossing occurs at $\omega_c = \omega_0/\sqrt{2}$, which for $\hbar\omega_0 \approx 3$ meV,³ yields just $B = 1.2$ T. Coupling of $|-1, 0; l_0, \alpha_0\rangle$ with $|2, 0; l_0, \alpha_0\rangle$ requires, however, a confinement potential that lacks inversion symmetry (e.g., $\propto x^3$). This has no experimental justification. Coupling with, e.g., $|2, 0; l_0 - 3, \alpha\rangle$ is possible by a circular symmetric correction cr^6 . The high energy of the RM in this state excludes, however, an anticrossing.

In the quadratic array of dots investigated by Demel *et al.*, a correction $\propto (x^2y^2 - r^4/8)$ to the confinement potential is very likely to exist. In the decomposition analogous to Eq. (7), the pure CM part couples $|-1, 0; l_0, \alpha_0\rangle$ with $|3, 0; l_0, \alpha_0\rangle$, which has the same energy for $\omega_c = 2\omega_0/\sqrt{3}$. With $\hbar\omega_0 \approx 3$ meV,³ this yields $B = 2.0$ T, and the corresponding matrix element is too small ($\propto N^{-1}$) to make this anticrossing observable. The term corresponding to H_{22} , however, couples $|-1, 0; l_0, \alpha_0\rangle$ to a state of the form $|1, 0; l_0 + 2, \alpha\rangle$, and the coupling matrix element does not become small with increasing N . Without Coulomb interaction, $|1, 0; l_0 + 2, \alpha_0\rangle$ would be degenerate with $|3, 0; l_0, \alpha_0\rangle$. For the interacting system, however, $|1, 0; l_0 + 2, \alpha_0\rangle$ has a lower energy, since its RM part has a larger spatial extent, and leads to an anticrossing at a lower B value than 2.0 T.

To get information about the energy dispersion of excited eigenstates, we calculated the collective RPA response of the parabolically confined system to external fields with different angular momenta N_p . The results are shown in Fig. 4 and reveal the unique role played by the dipole transitions ($N_p = \pm 1$) which leave the state of the RM invariant. All other modes have lower frequencies than expected from the single-particle picture, indicating that excited states of the RM are involved. The pure CM transitions with $N_p = 0, \pm 2$, and ± 3 have dispersions $\omega = \tilde{\omega}$, $\tilde{\omega} \pm \omega_c$, and $\frac{3}{2}(\tilde{\omega} \pm \omega_c)$, respectively, and are not excited (note $\tilde{\omega} = 6.74$ meV at $B = 0$). Our interpretation is that, for $N_p = \pm 2$, the main transitions go to final states of the form $|\pm 1, 0; l_0 \pm 1, \alpha\rangle$, and the weaker ones (with increasing dispersion near 4 meV) to $|0, 0; l_0 - 2, \alpha\rangle$. Similar, for $N_p = \pm 3$, the final states are of the form $|\pm 2, 0; l_0 \pm 1, \alpha\rangle$ for the main transitions, and two weaker transitions to states with higher angular momentum of the RM are resolved. The monotonically decreasing branch with $N_p = 3$ crosses the increasing dipole

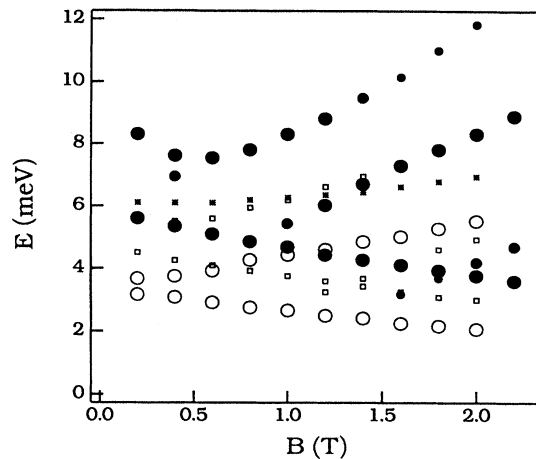


FIG. 4. The excitation spectra for the following: *, the $N_p = 0$; o, the $N_p = \pm 1$; □, the $N_p = \pm 2$; and ●, the $N_p = \pm 3$ modes. The $N_p = 0, \pm 2$ modes are shown with small symbols, but the symbol size for $N_p = -3$ indicates the relative strength of the absorption.

branch with $N_p = -1$ near $B = 1.2$ T. The corresponding final states, $|2, 0; l_0 + 1, \alpha\rangle$ and $|-1, 0; l_0, \alpha_0\rangle$, are coupled by the perturbation $(x^2y^2 - r^4/8)$ discussed above. This leads to an anticrossing near $B = 1.2$ T, which should be observable in the dipole excitation. For the parameter values of Fig. 4, an anticrossing due to the pure CM excitation to the state $|3, 0; l_0, \alpha\rangle$, which is not seen in the RPA, would occur near the higher magnetic field $B = 2.2$ T.

In summary, our RPA calculations together with analytical arguments provide a good qualitative understanding of the recent FIR experiments by Demel *et al.*³ A circular symmetric correction, that makes the confinement steeper than the parabolic one, leads to a blue shift of the dipole modes increasing slightly with the electron number N in the dot, and in addition to the appearance of a higher mode. To explain the observed anticrossing, one needs a deviation from the circular symmetry. In all cases the coupling of the center of mass and the relative motion by the deviations from the parabolic confinement potential is essential.

We acknowledge stimulating discussions with T. Demel, D. Heitmann, D. Pfannkuche, and E. Zaremba. This research was supported in part by the Icelandic Natural Science Foundation.

¹S.J. Allen, H.L. Störmer, and J.C.M. Hwang, Phys. Rev. B **28**, 4875 (1983).

²Ch. Sikorski and U. Merkt, Phys. Rev. Lett. **62**, 2164 (1989).

³T. Demel, D. Heitmann, P. Grambow, and K. Ploog, Phys. Rev. Lett. **64**, 788 (1990).

⁴A.L. Fetter, Phys. Rev. B **32**, 7676 (1985); **33**, 5221 (1986).

⁵V. Shikin, S. Nazin, D. Heitmann, and T. Demel, Phys. Rev. B **43**, 11 903 (1991).

⁶P.A. Maksym and T. Chakraborty, Phys. Rev. Lett. **65**,

108 (1990).

⁷P. Bakshi, D.A. Broido, and K. Kempa, Phys. Rev. B **42**, 7416 (1990).

⁸Tapash Chakraborty, V. Halonen, and P. Pietiläinen (unpublished).

⁹V. Gudmundsson, Solid State Commun. **74**, 63 (1990).

¹⁰V. Fock, Z. Phys. **47**, 446 (1928).

¹¹D.A. Broido, K. Kempa, and P. Bakshi, Phys. Rev. B **42**, 11 400 (1990).

¹²W. Que and G. Kirczenow, Phys. Rev. B **38**, 3614 (1988).